JOURNAL OF MATERIALS SCIENCE **33** (1998) 4375–4379

Discrete β-Ta_2O_5 crystallite formation in reactively sputtered amorphous thin films

P. J. BECKAGE*, D. B. KNORR†, X. M. WU§, T.-M. LU, E. J. RYMASZEWSKI
Center for Integrated Electronics and Electronics Manufacturing, Rensselaer Polytechnic Institute, Troy, NY 12180, USA
E-mail: knorr@worldnet.att.net

The crystallization of thin amorphous TaO_x films formed by d.c. reactive sputtering was investigated at temperatures from 500–700 °C. The films remained amorphous for times up to 100 h at 500 °C. The formation of discrete, single crystallites of the orthorhombic β-Ta_2O_5 phase was observed after annealing at 600 °C for times from 8–108 h. The crystallites were 0.35 μm × 0.35 μm after 8 h and grew to approximately 2.5 μm × 2.0 μm after 108 h. A (2 0 0) fibre texture with a 6° spread was observed. More rapid in-plane growth in the [0 1 0] direction resulted in a near-rectangular shape and is attributed to a ledge growth mechanism. Higher temperature anneals at 650 and 700 °C produced less-textured polycrystalline films with remnant amorphous regions. © *1998 Kluwer Academic Publishers*

1. Introduction

Thin ceramic films are being pursued as a dielectric in a variety of solid-state applications [1, 2]. Ta_2O_5 is one such candidate material that is considered in this paper. A variety of properties is important to the performance and reliability of such dielectric films [3, 4]: dielectric constant [2], loss tangent, breakdown strength, and leakage current. The microstructure from the unit-cell scale to a length scale of the order of the film thickness strongly affects these properties. Examples of important attributes are defect structures and chemistry (e.g. Ta/O ratio). Because the films can be deposited in either amorphous or crystalline forms, the extent of crystallinity is fundamental to the behaviour of these films.

Processing studies have used several techniques to grow Ta_2O_5 thin films: reactive sputtering [1–6], tantalum evaporation followed by thermal oxidation [7], sputtered tantalum followed by anodization [8–10], and chemical vapour deposition (CVD) [11, 12]. The highest processing temperature that retains the amorphous structure depends on the method of deposition: 300–350 °C for reactive sputtering [1, 2], and 600 °C for metalorganic CVD [11]. Room-temperature reactive sputtering always produces an amorphous structure [1–4], while anodization of tantalum results in "microcrystalline" regions [8, 9]. For thermal treatments subsequent to deposition, the only evidence cited for the crystallization of amorphous Ta_2O_5 below 600 °C was for a 580 °C/15 h anneal [7].

In the present work, the crystallization of amorphous, reactively sputtered thin films of Ta_2O_5 has been investigated. The morphology of the crystallized regions has been correlated with annealing time at 600 °C, and the kinetics of the crystallization process were deduced and related to the crystallite morphology. The crystallographic anisotropy of the crystallites has been emphasized, and crystallization behaviour at higher temperatures was briefly considered.

2. Experimental procedures

Amorphous TaO_x thin films were deposited on (1 0 0) silicon wafers by a reactive d.c. sputtering technique [6]. Argon and oxygen were introduced directly into the chamber to give a total gas flow of 10 standard $cm^3 min^{-1}$. The Ar/O_2 ratio was fixed to produce a TaO_x stoichiometry near Ta_2O_5. Deposition parameters were a base vacuum pressure of 5.3×10^{-4} Pa prior to deposition and a 3 Pa (23 m torr) working gas pressure during the deposition. The sputtering voltage was 1000 V, and the plasma current was 50 mA. Although there was no intentional substrate heating, the substrate temperature was measured to be approximately 10 °C lower than the target temperature, which was 190–200 °C. The film thickness was 60–250 nm as measured by ellipsometry following the deposition. The most extensive annealing study was done at 600 °C on a 100 nm film.

The post-deposition heat treatments were performed in air using a Thermolyne Type 48000 Furnace with a ramp rate of approximately 20 °C min^{-1}. Conditions were temperatures of 500, 600, 650, and 700 °C

* *Present address*: Advanced Micro Devices, Austin, TX, USA.
† *Present address*: Lockheed-Martin, Schenectady, NY, USA.
§ *Present address*: Analog Devices, Inc., Wilmington, MA, USA.

for time intervals of 0.5–108 h. A separate sample was used for each annealing temperature, but at a particular temperature, the same sample was annealed at successive times. Bragg–Brentano X-ray diffraction scans were obtained on a Scintag PTS 2000 diffractometer. Texture was determined on a Siemens pole figure diffractometer using the Schultz reflection technique [13]. All X-ray diffraction analyses used CuK_α radiation. Samples for transmission electron microscopy (TEM) were prepared by standard techniques, including ion milling, and examined in a Jeol JEM-100CX II electron microscope at an operating voltage of 100 kV by both bright-field illumination and selected-area diffraction.

Figure 1 Bright-field transmission electron micrograph of 100 nm thick Ta_2O_5 film annealed for 24 h at 600 °C. The film is primarily amorphous with some square to slightly rectangular crystallites.

3. Results and discussion
3.1. General observations
The film crystallinity following anneals at various temperatures is summarized in Table I. The most unique finding was the presence of discrete, individual crystallites of β-Ta_2O_5, which had nucleated and grown after an 8 h anneal at 600 °C. Initially, the crystallites were nearly square in shape (Fig. 1 shows the crystallites after 24 h) but became progressively rectangular ("bow-tie" shaped) for longer annealing times up to 108 h (Fig. 2a).

Crystallization greatly accelerates with increasing temperature where the crystalline fraction is substantial after 4 h at 650 °C and is essentially complete after 0.5 h at 700 °C. Although most of the film volume at 700 °C is polycrystalline, the presence of amorphous regions, as seen in Fig. 3, is confirmed by selected-area diffraction. Bragg–Brentano scans for 650 and 700 °C samples reveal multiple diffraction peaks between 2θ angles of 20° and 50°, indicating that a strong texture is no longer present. Multiple diffraction peaks have also have observed for films processed at higher temperatures by CVD [11], by high-temperature reactive sputtering [1, 2], and by reactive sputtering followed by annealing [7]. In addition, a strong texture forms at the lowest processing temperature to produce a crystalline film. A change in nucleation mechanism from one dominant orientation at low crystallization temperature to multiple orientations at high temperatures, might be responsible.

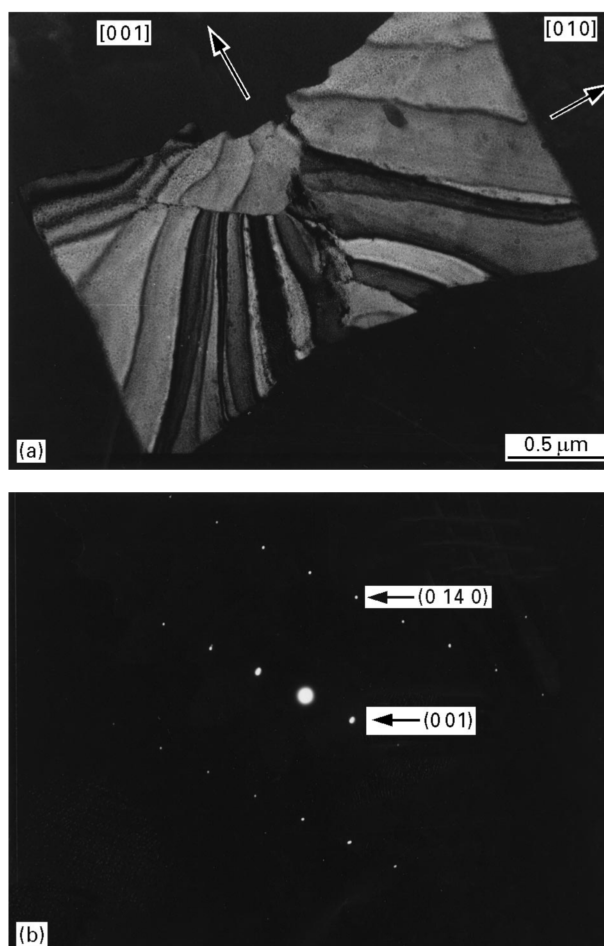

Figure 2 Near rectangular ("bow-tie") crystallite of Ta_2O_5 formed by an anneal at 600 °C for 108 h. (a) Bright-field showing crystallographic orientation along the major axes; (b) selected-area diffraction of the crystallite, which was used to determine the orientation.

3.2. Crystallography
An early study [14] interpreted the X-ray diffraction data for the low-temperature Ta_2O_5 phase, commonly referred to as either β-Ta_2O_5 or L-Ta_2O_5, as equivalently orthorhombic and monoclinic. Subsequent

TABLE I Summary of results on the formation of β-Ta_2O_5

Temperature (°C)	Time (h)	Thickness (nm)	Results
500	4–100	60	Amorphous
600	2–4	100	Amorphous
600	8–108	100	Discrete crystals in amorphous matrix
650	4	250	Polycrystalline with amorphous regions
700	0.5	55	Polycrystalline with amorphous regions

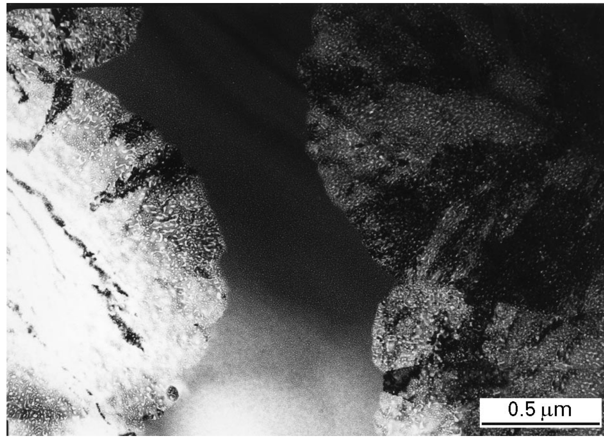

Figure 3 Bright-field transmission electron micrograph for an anneal of 0.5 h at 700 °C. A crystallized area split by an amorphous band is shown.

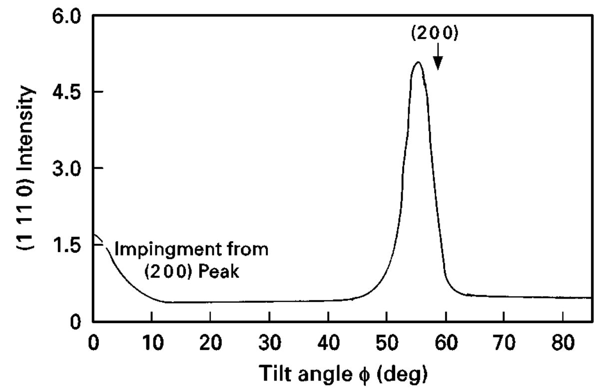

Figure 4 (1 11 0) fibre texture plot of Ta_2O_5 film annealed for 76 h at 600 °C.

work has used either the monoclinic notation [1, 2] or the orthorhombic notation [4, 7, 11, 12] to represent the low-temperature Ta_2O_5 phase. Two studies [14, 15] defined an orthorhombic subcell with approximate lattice parameters of $a' = 0.620$ nm, $b' = 0.366$ nm, and $c' = 0.389$ nm. The lattice parameters for the complete unit cell [15, 16] are $a = 0.620$ nm, $b = 0.429$ nm, and $c = 0.389$ nm. Furthermore, the b lattice parameter varies by a multiplicative factor of 11 or 14 relative to the subunit cell size [17]. Williams and co-workers [18–20] have studied the variation in the b lattice parameter with the addition of Al_2O_3, TiO_2, ZrO_2, WO_3, or HfO_2 and were able to correlate the lattice constant variations with temperature, deposition conditions, and impurity content. The orthorhombic crystal structure is presumed in this study, so all crystallographic indices will be based on the a, b, and c lattice parameters.

Because a variation in the b lattice parameter is reported [18–20], the interplanar spacing was determined from multiple electron diffraction patterns of discrete single crystallites. The value of the b lattice parameter ranges from 3.7353 to 4.2120 nm with an average of 3.999 nm. In relation to the reported subcell lattice parameter of $b = 0.366$ nm, a multiplicative factor between 10.2 and 11.5 is calculated. This is in reasonable agreement with the reported literature multiplicative values of 11–14 [18–20]. Although a range of b lattice parameters was observed, the average was only $\sim$0.7% lower than the currently accepted value of 4.029 nm [16].

3.3. Crystallite texture

Specific crystallographic relationships are associated with the nucleation and growth of the Ta_2O_5 crystallites at 600 °C. From the Bragg–Brentano scans, only the (2 0 0) planes at $2\theta = 28.8°$ diffract, indicating that these planes must be oriented parallel to the substrate/film surface; this relationship was confirmed by TEM. The spread of the (2 0 0)-oriented crystallites in a sample annealed for 76 h was measured by texture analysis. An (1 11 0) pole figure scan was obtained, but the proximity of several other diffraction peaks [16] means that signals from the nearby peaks might contribute. Despite the crystallization on a single-crystal substrate, no in-plane orientation of the crystallites was found. The presence of a fibre texture is supported by the TEM observations of discrete crystallites with random in-plane orientation. The texture results are presented in Fig. 4 as a fibre texture plot [21, 22], where the tilt angle ϕ is 0° normal to the film and 90° in the plane of the film. The results show a strong (1 11 0) orientation at a tilt angle of 56°, which is close to the 59° interplanar angle between (2 0 0) and (1 11 0). The smaller component about $\phi = 0°$ represents some impingement of the (2 0 0) peak, which is expected to contribute at that location for a (2 0 0) fibre texture. The presence of the (1 11 0) planes was verified with TEM electron diffraction by rotating off the 0° tilt angle. A tight (2 0 0) orientation distribution with a spread about the ideal orientation of approximately 6° is observed. Other studies [1, 2] of reactively sputtered films have used Bragg-Brentano peaks to infer a dominant (2 0 0) texture.

The β-Ta_2O_5 phase appears as discrete crystallites in an otherwise amorphous matrix, so selected-area diffraction is able to establish the in-plane crystallographic directions associated with crystallite edges. A transmission electron micrograph (Fig. 2a) and corresponding electron diffraction pattern (Fig. 2b) were directly compared using a rotation calibration, which resulted in the [0 0 1] and [0 1 0] directions indicated on Fig. 2a. Thus, the *macroscopic* growth rate of [0 1 0] exceeds that of [0 0 1]. The growth anisotropy is quantified by plotting the time dependence of the length and the width dimension in Fig. 5. The growth rate is 10.3 and 5.1 nm h^{-1} for [0 1 0] and [0 0 1], respectively. After 108 h, faceting along the crystallite edge is apparent as wide steps and short step heights. The crystallites are much larger than the thickness of the film, even for short times and low fractions of crystallization, so the growth is two-dimensional.

3.4. Crystallization kinetics

After 100 h at 500 °C, a 60 nm film remains amorphous as confirmed both by TEM electron diffraction and by X-ray diffraction. At 600 °C, no crystallization was evident in a 100 nm film after 4 h, but discrete single

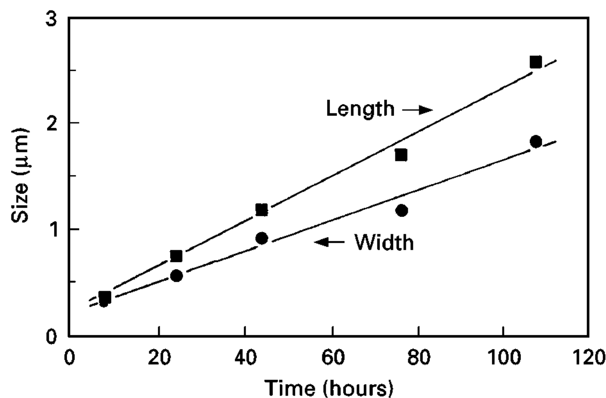

Figure 5 Dimensions of crystallites along major directions for anneals at 600 °C.

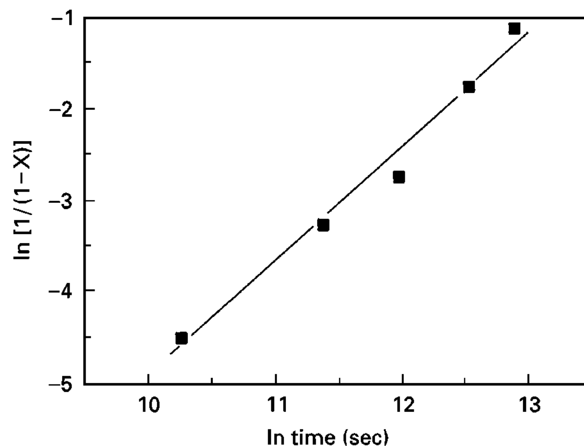

Figure 6 Plot of crystallization data from Table II to determine the exponent in the Johnson–Mehl–Avrami equation.

TABLE II Crystallite formation in β-Ta_2O_5 at 600 °C

Annealing time (h)	Area crystallized (%)	Crystallite number density (μm^{-2})
8	1.1	0.13
24	3.8	0.12
44	6.3	0.06
76	16.0	0.10
108	28.2	0.05

crystallites extending through the film thickness were apparent after 8 h. This implies that the time to grow a nucleus through the film thickness at 600 °C is short. The number density decreased slightly for anneals up to 108 h, as seen in Table II, which could be due to the growth of some existing crystallites to impingement as the crystallized volume fraction increases. The growth data at 600 °C were fit to the Johnson–Mehl–Avrami (JMA) equation [23–26]

$$X = 1 - \exp(-Kt^n) \quad (1)$$

where X is the fraction crystallized, K is a temperature-dependent scaling factor which carries the activation energy, t is time, and n is a time exponent. The JMA plot is shown in Fig. 6, where n is calculated to be 1.3, and $K = 2 \times 10^{-8}$.

The exponent in the JMA equation often reflects the kinetic process(es) that is/are occurring [27]. Because the number density of crystallites does not increase with time, a condition of site saturation (zero nucleation rate during growth) exists. Furthermore, interface-controlled growth should dominate, because no long-range diffusion is involved. A rearrangement at the crystallite/amorphous matrix interface most likely occurs, given the structural similarity of amorphous tantalum oxide compared to the crystalline form [10]. The exponent is now expected to scale with the dimensionality of growth [28], i.e. n is 3, 2, or 1 for three-dimensional, two-dimensional, or one-dimensional growth, respectively. Such behaviour was demonstrated for three-dimensional crystallization with site saturation in cordierite [29], where $n = 3$ was found. In this study, the growth of the crystallites is quasi-one-dimensional. Ledges or steps nucleate at the amorphous/crystalline interface and propagate laterally along the interface. The processes along the macroscopically faster growing (0 1 0) face are controlling, where easy nucleation of (0 1 0)-faced ledges and/or rapid propagation of the ledge along the [0 0 1] direction occur. The "bow-tie" shape develops because the termination of ledges at the corner extends the short dimension of the crystallite. The roughness and steps observed along the [0 0 1] face in Fig. 2a support this interpretation. Thickening in the [0 0 1] direction occurs both as a consequence of the [0 1 0] face growth and by the nucleation of (0 0 1)-faced steps and their propagation along [0 1 0]. Clearly, the latter process on the (0 0 1) face is more difficult and slower than along the faster growing (0 1 0) face.

The {0 0 1} interfaces have substantially lower interfacial energy than other crystallographic orientations. The substrate/TaO_x(1 0 0) and/or ambient/TaO_x (1 0 0) is preferred for crystallite nucleation at 600 °C. The cusp of the interfacial energy orientation dependence on the Wulff plot must be quite deep and sharp because of the modest 6° spread about (1 0 0). Likewise, the (0 1 0) and (0 0 1) faces, interfaced with amorphous TaO_x, have minima in interfacial energy. The equilibrium crystallite shape should reflect the ratio of interfacial energies, i.e. $\gamma_{(001)}/\gamma_{(010)} \sim 1.3$. However, the differences in interfacial nucleation and growth means that the equilibrium shape is not achieved. A relationship $\gamma_{(001)} \sim \gamma_{(010)}$ is more likely, given the nearly square shape of the crystallites soon after nucleation. The aforementioned kinetic growth factors are responsible for the non-equilibrium shape [30].

The nucleation event was not isolated in this study, so it is not known whether nucleation occurs at the ambient/film or the silicon/film interface. However, surface nucleation is inferred because the random in-plane crystallite orientation lacks a substrate influence. If the crystallites nucleated at the Si(0 0 1) interface, some in-plane orientation might be expected. Furthermore, surface nucleation resulting in a preferred orientation is an established mechanism in the crystallization of glass-ceramics [31].

Cracks in the crystallites, but not in the amorphous regions, were commonly observed and are seen in Fig. 2a as discontinuities in the thickness fringes. The films are under a high tensile stress in the as-deposited condition, which becomes greater as crystallization proceeds [32]. Volume contraction due to reduction of free volume during crystallization could contribute to the high stress [33]. Steps and other discontinuities could also concentrate the stress, serving as crack initiation sites. Defects such as pinholes [5] and cracks [4] are known to develop after annealing at temperatures high enough to induce crystallization. A consequence of the cracks is a substantial decrease in dielectric strength.

4. Conclusion

The formation of discrete β-Ta_2O_5 crystallites occurred by annealing a reactively sputtered film in air at 600 °C for times between 8 and 108 h. The crystallites were nearly rectangular in shape and extended through the thickness of the 100 nm films. The preferred orientation of the crystallites was (2 0 0) in a fibre texture with a 6° spread. An in-plane slow growth direction of [0 0 1] was found for discrete crystallites. Growth was quasi-one-dimensional and followed Johnson–Mehl–Avrami kinetics with a time exponent of 1.3. For a 100 h anneal at 500 °C, the films remained completely amorphous. At higher temperatures of 650 and 700 °C, the films were polycrystalline due to the impingement of the discrete crystallites with some residual amorphous regions. The behaviour of Ta_2O_5 films in this study is consistent with other studies on Ta_2O_5 films, indicating that crystallization behaviour is not very sensitive to the specific deposition conditions.

Acknowledgements

The authors would like to thank Dr. D. P. Tracy for the texture analysis and the Electron Microscopy group at RPI for their assistance. We also acknowledge valuable discussions with Dr. W. -T. Liu. This work was supported by ARPA under Contract Number ONR N00014-91J-4012, which is gratefully acknowledged.

References

1. C. GUOPING, L. LINGZHEN, Z. SUIXIN and Z. HASKANG, *Vacuum* **41** (1990) 1204.
2. Y. NAKAGAWA, Y. GOMI and T. OKADA, *J. Appl. Phys.* **61** (1987) 5012.
3. Y. NISHIOKA, N. HOMMA, H. SHINRIKI, K. MUKAI, K. YAMAGICHI, A. UCHIDA, K. HIGETA and K. OGIUE, *IEEE Trans. Electron Dev.* **ED-34** (1987) 1957.
4. S. ROBERTS, J. RYAN and L. NESBIT, *J. Electrochem. Soc.* **133** (1986) 1405.
5. S. KIMURA, Y. NISHIOKA, A. SHINTANI and K. MUKAI, *ibid.* **130** (1983) 2414.
6. X. M. WU, P. K. WU, T. -M. LU and E. J. RYMASZEWSKI, *Appl. Phys. Lett.* **62** (1990) 1204.
7. G. S. OEHRLEIN, F. M. D'HEURLE and A. REISMAN, *J. Appl. Phys.* **55** (1984) 3715.
8. K. SHIMIZU, G. E. THOMPSON, G. C. WOOD and K. KOBAYASHI, *Philos. Mag. B* **63** (1991) 891.
9. B. W. SHEN, I. C. CHEN, S. BANERGEE, G. A. BROWN, J. BOHLMAN, P. H. CHANG and R. R. DOERING, *IEEE IEDM* (1987) 582.
10. L. A. ALESHINA, V. P. MALINENKO, A. D. PHOUPHANOV and N. M. JAKOVLEVA, *J. Non-Cryst. Solids* **87** (1986) 350.
11. K. TOMINAGA, R. MUHAMMET, I. KOBAYASHI and M. OKADA, **31** (1992) 585.
12. W. H. KNAUSENBERGER and R. N. TAUBER, *J. Electrochem. Soc.* **120** (1973) 927.
13. L. G. SCHULTZ, *J. Appl. Phys.* **20** (1949) 1030.
14. N. TERAO, *Jpn J. Appl. Phys.* **6** (1967) 21.
15. R. S. ROTH, J. L. WARING and H. S. PARKER, *J. Solid State Chem.* **2** (1970) 445.
16. Card 25-922, (Joint Committee on Powder Diffraction Standards – International Centre for Diffraction Data, Swarthmore, PA, 1991).
17. N. C. STEPHENSON and R. S. ROTH, *Acta Crystallogr.* **B27** (1970) 1037.
18. J. M. WILLIAMS, R. J. D. TILLEY, G. HARBURN and R. P. WILLIAMS, *J. Solid State Chem.* **92** (1991) 460.
19. G. HARBURN, R. J. D. TILLEY, J. M. WILLIAMS, R. P. WILLIAMS and J. HUTCHISON, *J. Chem. Soc. Farad. Trans.* **88** (1992) 621.
20. J. M. WILLIAMS, R. J. D. TILLEY, G. HARBURN and R. P. WILLIAMS, *ibid.* **88** (1992) 325.
21. D. B. KNORR, in "Materials Reliability Issues in Microelectronics III", Vol. 309, edited by K. P. Rodbell, W. F. Filter, H. J. Frost and P. S. Ho (Materials Research Society, Pittsburgh, PA, 1993) p. 75.
22. D. B. KNORR and J. A. SZPUNAR, *JOM* **46** (9) (1994) 42.
23. W. A. JOHNSON and R. F. MEHL, *Trans. AIME* **135** (1939) 411.
24. M. AVRAMI, *J. Chem. Phys.* **7** (1939) 1103.
25. *Idem, ibid.* **8** (1940) 212.
26. *Idem, ibid.* **9** (1941) 177.
27. J. W. CHRISTIAN "The Theory of Transformations in Metals and Alloys" (Pergamon, New York, 1965) Ch. 12, p. 471.
28. J.-H. JEAN and T. K. GUPTA, *J. Mater. Res.* **7** (1992) 3103.
29. B. C. LIM and H. M. JANG, *ibid.* **6** (1991) 2427.
30. M. FERRANTE and R. D. DOHERTY, *Acta Metall.* **27** (1979) 1603.
31. P. W. McMILLAN, "Glass-Ceramics", 2nd Ed (Academic Press, New York, 1979) p. 150.
32. P. J. BECKAGE, MS thesis, Rensselaer Polytechnic Institute, August 1993.
33. H. HOSONO, Y. SHIMIZU, H. OHSATO and Y. ABE, *J. Mater. Sci. Lett.* **6** (1987) 394.

Received 14 November 1997
and accepted 15 May 1998